Real-time monitoring of ruling grating resolution by digital wavefront

Chao Yang,[1,2,*] Haili Yu,[1] Xiaotian Li,[1] Jicheng Cui,[1] Bayanheshig,[1] Xiangdong Qi,[1] and Yuguo Tang[1]

[1]Grating Technology Laboratory, Changchun Institute of Optics and Fine Mechanics and Physics, Chinese Academy of Sciences, Changchun, Jilin 130033, China

[2]College of Physics, University of Chinese Academy of Sciences, Beijing 100049, China

*Corresponding author: yangchaoby@usina.com

Received 28 August 2014; revised 9 November 2014; accepted 26 November 2014; posted 26 November 2014 (Doc. ID 221808); published 15 January 2015

In order to solve the problem that the grating quality cannot be monitored directly in real time, we provided a method based on Rayleigh criterion with our designing optical measurement structure to measure yaw and displacement errors of a grating ruling machine feeding system. Gratings are ruled with or without errors correction by the real-time monitoring system . It shows that the resolution obtained without errors correction is reduced from 99.97% to 87.47% of theoretical value, while the resolution obtained with errors correction is stable, remaining at 99.99%–97.21%. The experimental result is that the grating quality can be guaranteed by monitoring grating resolution in real time.

OCIS codes: (050.1950) Diffraction gratings; (120.5050) Phase measurement; (220.4830) Systems design; (350.5730) Resolution.

http://dx.doi.org/10.1364/AO.54.000492

1. Introduction

Plane diffraction gratings [1], which have excellent optical functions such as polychromatic light dispersion, polarization, and phase matching, are very popular for military, astronomy, defense, and civilian applications [2–4]. These gratings are mainly produced by mechanical ruling and ion-beam etching [5]. Until now, because of deep grooves with strict shapes, echelles and infrared-laser gratings are still produced by mechanical ruling [6].

In mechanical ruling, it takes a long time to rule each grating especially for a large size grating. At the same time there are a lot of errors such as diamond tool wear, environment factors, testing accuracy errors and so on [7–9]. Many scholars have studied how to enhance pitching accuracy of the grating engine [10–12]. MIT applied an interferometer as a measuring and feedback element, with a motor as an executing element driving the inside carriage to the ruling engine, correcting the yawing errors to 0.02 in [13]. Japanese researchers used a piezoelectric actuator as an executing element to correct ruling errors, improving the ruling accuracy [14].

Because of the strict ruling accuracy, the grating ruling engine has to be placed in a sealed room in order to maintain a high ruling accuracy and a perfect environment condition including temperature, humidity, and vibration [13]. However, even in this condition it is quite difficult to ensure the ruling quality after hundreds of ruling hours unless the grating quality can be monitored in real time. As the grating constant is between micrometer and nanometer scale, the grating surface is covered with an oil film, the spectral performance such as wavefront quality, resolution, and scattered light cannot be read out directly. In this paper, we proposed a method

1559-128X/15/030492-06$15.00/0

to monitor the grating quality in real time by digital wavefront.

This paper is organized as follows. In Section 2, the basic theory of grating quality is monitored in real time. In Section 3, we apply the above technique to the actual experiment and the relative result is introduced. The conclusion is given in Section 4.

2. Theory

A. Resolution Calculation

Errors of ruling are a determining factor impacting on grating quality. The errors matrix can be written as

$$\delta_{ab} = \begin{bmatrix} \delta_{11} & \delta_{21} & \cdots & \delta_{n1} \\ \delta_{12} & \delta_{22} & \cdots & \delta_{a2} \\ \vdots & \vdots & \ddots & \vdots \\ \delta_{1b} & \delta_{2b} & \cdots & \delta_{ab} \end{bmatrix}. \tag{1}$$

The optical path difference is as follows:

$$\delta = \delta_{r1} + \delta_{r2} = \delta_{ab} \times (\sin\theta_{1b} + \sin\theta_{2b}). \tag{2}$$

The grating diffraction equation is given by

$$d(\sin\theta_{1m} + \sin\theta_{2m}) = m\lambda. \tag{3}$$

d is grating constant; θ_i is incidence angle; θ_m is refraction angle and m is diffraction order; λ is incidence wavelength. From formulas (2) and (3), the wavefront error Δm is given as

$$\Delta_m = \frac{m}{d}\begin{bmatrix} \delta_{11} & \delta_{21} & \cdots & \delta_{n1} \\ \delta_{12} & \delta_{22} & \cdots & \delta_{a2} \\ \vdots & \vdots & \ddots & \vdots \\ \delta_{1b} & \delta_{2b} & \cdots & \delta_{ab} \end{bmatrix}. \tag{4}$$

We assume that for a plane grating, the normalized coordinates of the diffraction angle spectrum are u and v respectively, the normalized grating diffraction wavefront along coordinates x, y of the pupil are $\eta(|\eta| \le 1)$ and $\xi(|\xi| \le 1)$. In this case, the amplitude distribution of the diffraction spectrum is given by

$$E(u,v) = C\int_{-1}^{1}\int_{-1}^{1} E_0(\eta,\xi)\exp[ik\Delta(\eta,\xi)]\exp[i(u\eta + v\xi)]\mathrm{d}\eta\mathrm{d}\xi. \tag{5}$$

C is a constant and $\Delta(x,y)$ is the diffraction wavefront of the grating in the pupil. We consider that the amplitude of each point of the diffraction wavefront is equal, which means $E_0(\eta,\xi) = 1$. So we can get the normalized amplitude

$$A(u,v) = \frac{C\int_{-1}^{1}\int_{-1}^{1}\exp[ik\Delta(\eta,\xi)]\exp[i(u\eta+v\xi)]\mathrm{d}\eta\mathrm{d}\xi}{C\int_{-1}^{1}\int_{-1}^{1}\mathrm{d}\eta\mathrm{d}\xi} = \frac{1}{4}\int_{-1}^{1}\int_{-1}^{1}\exp[ik\Delta(\eta,\xi)]\exp[i(u\eta+v\xi)]\mathrm{d}\eta\mathrm{d}\xi. \tag{6}$$

According to two-dimensional fast Fourier transform, we can get the diffraction spectrum distribution, which is produced by discrete wavefront difference given by

$$A(u,v) = \frac{\mathrm{FFT}(\mathrm{FFT}(e^{ik\Delta_m})^T)^T}{nm} = \frac{\mathrm{FFT2}\{\exp[ik\Delta_m]\}}{ab}. \tag{7}$$

FFT is fast Fourier transform, while FFT2 is two-dimensional fast Fourier transform. The computation time can be reduced greatly by it. Based on the formula (7) and the Rayleigh criterion, suppose that Δu is the half-width of the first minimum angle, which is calculated by formula (7). We can get the grating resolution as follows:

$$\mathrm{RP} = \frac{\pi}{\Delta u} \times 100\%. \tag{8}$$

B. Error Source

Errors of ruling are produced by the ruling system, feeding system, and environmental factors. In order to maintain a perfect environment condition, the grating ruling engine should be placed in a sealed room.

The feeding system consists of a dividing motor, a worm gear, a lead screw-nut, lapped V-shaped monorail, and the working carriage. The working carriage consists of the inside carriage, outside carriage, parallel leaf spring, double piezoelectric actuators and springs, and the grating blank mounted on the inside carriage. Because of the straightness error of the lapped V monorail, and the machining errors of the gear, nut and screw, the working carriage will produce yaw and displacement errors when running a groove spacing, which will be impacted on the grating lines and bring about yaw and displacement errors, as shown in Fig. 1.

The ruling system consists of the crank link, copper slide, copper-slide guide, push-pull rod, saddle slider, fused-silica guide, and tool carriage. To produce the reciprocating motion of the diamond tool along the fused-silica guide, the crank link—driven by the ruling motor—moves the saddle slider across the fused-silica guide by a copper slide and push-pull rod. Pushing and pulling force will bring about deformation errors of the saddle slider and fused-silica guide, as shown in Fig. 2. Accordingly, errors of the ruling system are impacted on the groove straightness.

C. Simulation

Based on the above errors, we carried out a theory to analyze resolution in different conditions, such as

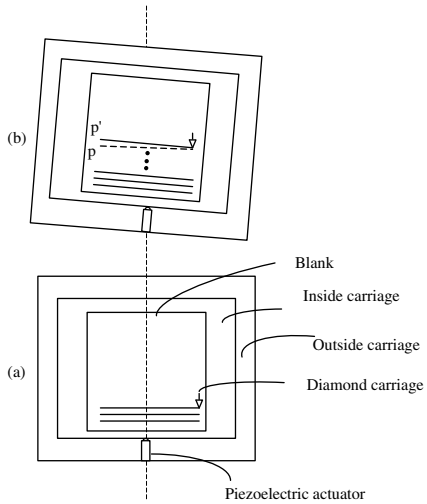

Fig. 1. Errors caused by feeding system.

adding yaw error, displacement error, and curvature error to grating lines.

First, we get the resolution curve considering random yaw errors in grating lines. Figure 3(a) shows resolution curve with a random yaw error in the range of 0.5 in. and Fig. 3(b) shows resolution curve with a random yaw error in the range of 0.1 in. We recorded resolution value every two groove lines. Abscissa represents record number while ordinate represents resolution. It can be seen that if yaw error is in the range of 0.5 in., the initial resolution curve is flat, with the enlarging of the ruling area, the resolution value is reduced from 97.22% to 41.66%. If the yaw error is in the range of 0.1 in., the resolution value is decreased from 99.99% to 94.59%. There is a big influence on grating resolution caused by yaw error.

A comparison of resolution curves with different displacement errors is shown in Fig. 4, indicating that when there is a random displacement error of d/5 and d/10 in the feeding system, we get grating resolution. It can be seen that with the increasing of displacement error, the resolution value will decrease.

Deformation error of saddle slider and fused-silica guide are systematic errors, which produce curvature errors of grating lines. Curvature error is in the sagittal direction of the grating, and it does not affect grating resolution [8,15].

From the above analysis we can see that yaw errors in the grating lines have a serious influence in the grating resolution value, and displacement errors also impact on the resolution. When the curvature error is in the sagittal direction, we do not consider it when we calculate the resolution value. So we just need to measure feeding system errors to monitor grating resolution.

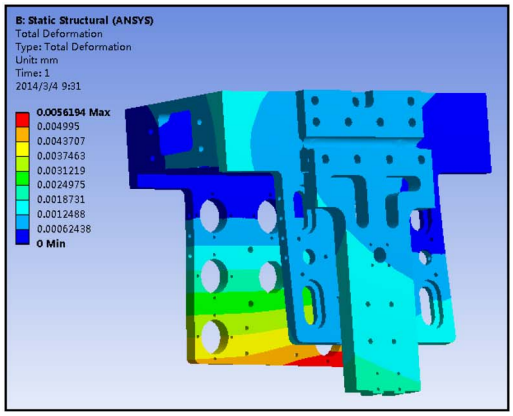

(a)

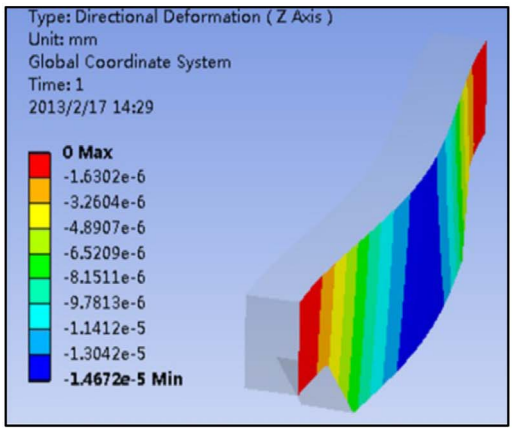

(b)

Fig. 2. Deformation caused by ruling system: (a) deformation of saddle slider; (b) deformation of fuse-silica guide.

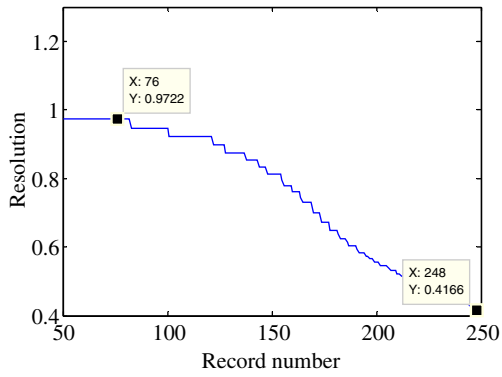

(a)

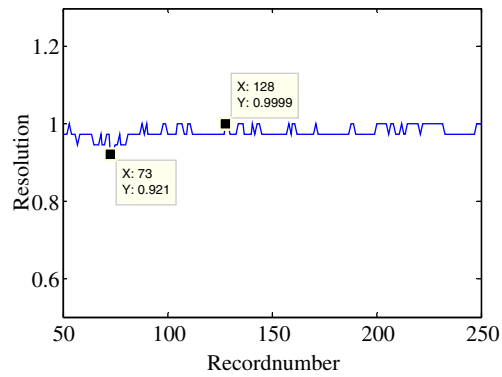

(b)

Fig. 3. Resolution curves with random yaw error: (a) 0.5 in. random yaw error; (b) 0.1 in. random yaw error.

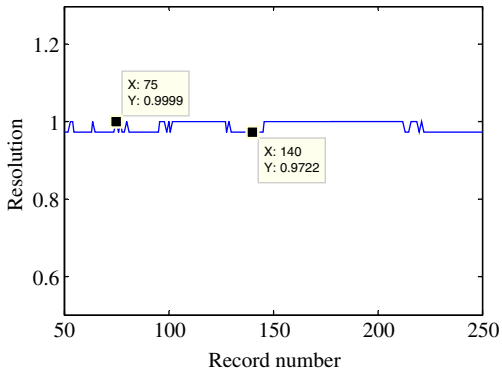

(a)

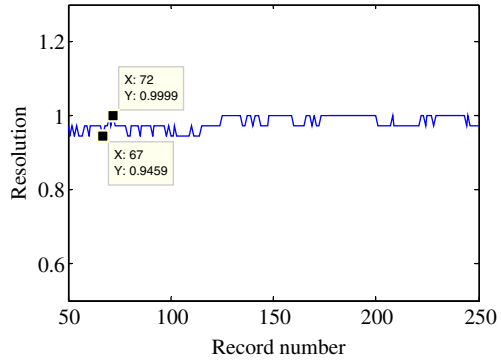

(b)

Fig. 4. Resolution curves with random displacement error: (a) d/10 random displacement error; (b) d/5 random displacement error.

D. Measuring System

Figure 5 shows the optical layout of the laser interferometer measuring feeding system errors in real time. A laser beam with $\lambda = 632.8$ nm is split into two parts by beam splitter A. Beam 1 incident to interferometer A and beam 2 incident to beam splitter B; beam 4 incident to the wavelength compensation interferometer in order to compensate errors that are produced by changing of refractive index air; beam 5 incident to interferometer B. When the dividing motor runs a groove space, the working carriage will produce an error; at the same time there will be an error adding to the bar mirror that is mounted on the inside carriage. Double piezoelectric actuators are used to correct errors of the inside carriage which are obtained by the optical path measurement. After getting the inside carriage errors, we adjust the length of the piezoelectric actuator to make the inside carriage in the ideal position. Finally, the pitch accuracy of the grating ruling machine reached 3 nm. In this situation, without error correction the yaw error is 0.2 in., while with error correction the yaw error was reduced to 0.02 in.

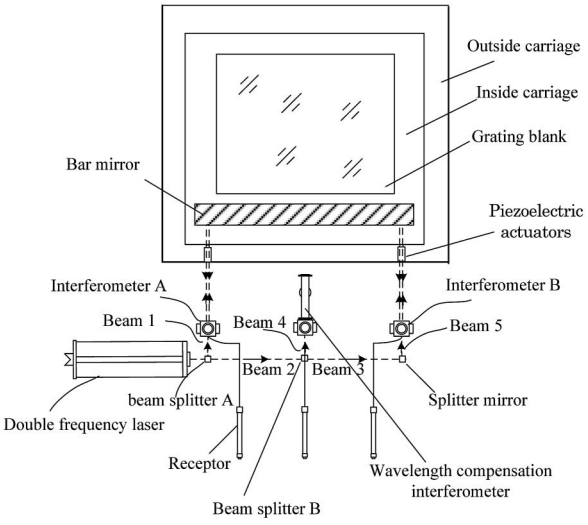

Fig. 5. Optical path measurement.

3. Experiment

In order to prove the availability of the real-time monitoring system, we used the CIOMP-2 grating ruling machine to rule two gratings with a line density of 600 line/mm. One grating was ruled without error correction, while the other with error correction. At the same time the grating resolution curves were monitored to judge the grating quality.

According to the theory model of the resolution and measuring system, we get groove error matrix δ_{ab} by the measure system. Putting errors into the model of real-time monitoring, we can get a theoretical resolution curve of the grating in real time. With the ruling area becoming larger and larger, we need more and more storage space to store the data and so resolution value is calculated every 10 lines. Each time it takes about 2–300 s with enlarging the grating size. After ruling 200 grooves we started recording the grating resolution.

Figure 6 shows the standard deviation value of the grating ruling machine when the grating ruling machine was ruled without error correction, abscissa representing the grating grooves and ordinate representing the standard deviation value. It can be seen that with the growing of grooves number, the accuracy of the ruling machine gradually gets worse, and the standard deviation value is 93.68 nm. In this way the resolution curve is shown in Fig. 7, where the resolution gradually reduced from 99.97% to 87.47%

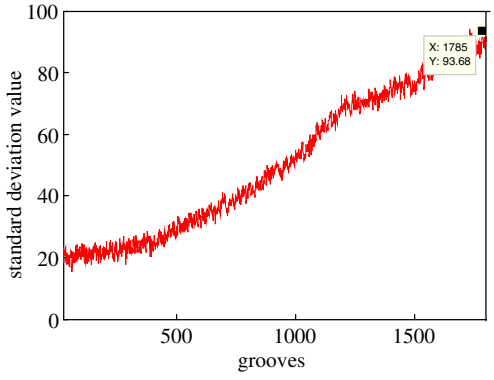

Fig. 6. Standard deviation value of the grating ruling machine.

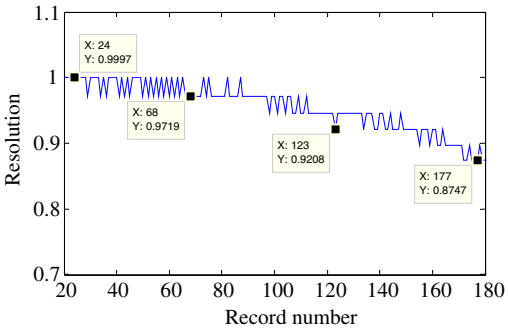

Fig. 7. Resolution curve without correction of the working carriage.

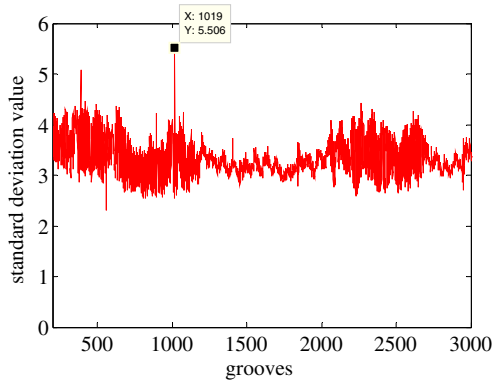

Fig. 8. Standard deviation value of the grating ruling machine.

of theoretical value. In the end of the curve, the resolution is lower than 90% of the theoretical value, which means the ruling can be stopped because the ruling quality cannot be promised in this situation.

Another grating is ruled with error correction. The standard deviation value of the grating ruling machine is shown in Fig. 8. It can be seen that the standard deviation value is about 5.5 nm, and it will not increase with the growing of grooves number. At the same time the resolution is stable within 99.99%–97.21% of the theoretical value, which is shown in Fig. 9. Comparing to the testing result without error correction in Fig. 7, the validity of the feeding system error correction model can be verified. During the entire ruling process, the resolution of the grating is always above 90% of theoretical value. With our technology, the actual resolution of the grating is 70%–80% of the theoretical analysis value.

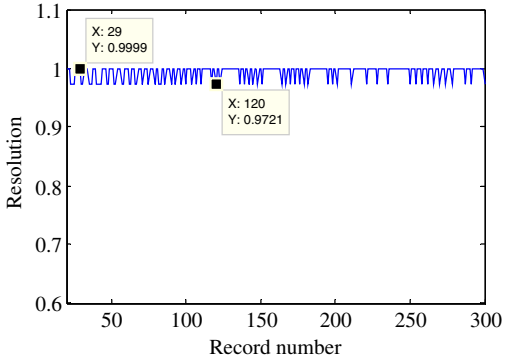

Fig. 9. Resolution curve with correction of the working carriage.

4. Conclusion

In this paper, we introduced a simple method for monitoring grating resolution in real time. We established a math model between grating resolution and errors of ruling. Based on the model we get that the main factors affecting the grating resolution are yaw and displacement errors, which are generated by the feeding system. In the latter part we designed a measuring optical path of the feeding system and carried out ruling experiments in different conditions. The experiment result showed that the resolution without errors correction was reduced from 99.97% to 87.47%, while with errors correction, the resolution curve stayed within the 99.99%–97.21% range. In conclusion, the method can get grating quality in real time by monitoring grating resolution, which means the grating ruling success rate will be improved significantly.

This work was supported by the National Basic Research Program of China (973 program), National Major and Research Equipment Development Project, Changchun Science and Technology Project, and Jilin Major Province Science and Technology Development Program Project.

References

1. H. D. Babcock, "Bright diffraction gratings," J. Opt. Soc. Am. **34**, 1–5 (1944).
2. F. M. Gerasimov, "Use of diffraction gratings for controlling a ruling engine," Appl. Opt. **6**, 1861–1864 (1967).
3. T. Jitsuno, S. Motokoshi, T. Okamoto, T. Mikami, D. Smith, M. L. Schattenburg, H. Kitamura, H. Matsuo, T. Kawasaki, K. Kondo, H. Shiraga, Y. Nakata, H. Habara, K. Tsubakimoto, R. Kodama, K. A. Tanaka, N. Miyanaga, and K. Mima, "Development of 91 cm size gratings and mirrors for LEFX laser system," J. Phys. **112**, 032002 (2008).
4. T. Suzuki, H. Kubo, T. Suganuma, T. Yamashita, O. Wakabayashi, and H. Mizoguchi, "High-resolution multigrating spectrometer for high quality deep UV light source production," Proc. SPIE **4346**, 1254–1261 (2001).
5. J. Flamand, F. Bonnemason, and A. Thevenon, "The blazing of holographic gratings using ion-etching," Proc. SPIE **1055**, 288–294 (1989).
6. H. D. Babcock and H. W. Babcock, "The ruling of diffraction gratings at the Mount Wilson Observatory," J. Opt. Soc. Am. **41**, 776–786 (1951).
7. G. R. Harrison, N. Sturgis, S. P. Davis, and Y. Yamada, "Interferometrically controlled ruling of ten-inch diffraction gratings," J. Opt. Soc. Am. **49**, 205–211 (1959).
8. X. Li, Bayanheshig, X. Qi, H. Yu, and Y. Tang, "Influence and revising method of machine-ruling grating line's curve error, location error on plane grating's performance," Chin. J. Lasers **40**, 0308009 (2013).
9. G. J. Dunning and M. L. Minden, "Scattering from high efficiency diffraction gratings," Appl. Opt. **19**, 2419–2425 (1980).
10. H. W. Babcock, "Control of a ruling engine by a modulated interferometer," Appl. Opt. **1**, 415–420 (1962).
11. C. Yang, H. Yu, X. Mi, Bayanheshig, and Y. Tang, "Yaw angle correction mechanism and experimental verification of large grating ruling machine," Chin. J. Sci. Instrum. **35**, 1065–1071 (2014).

12. E. Leibhardt, "Improved method for lapping a dividing gear for a ruling engine," J. Opt. Soc. Am. **42**, 447–450 (1949).
13. G. R. Harrison, S. W. Thompson, H. Kazukonis, and J. R. Connell, "750-mm ruling engine producing large gratings and echelles," J. Opt. Soc. Am. **62**, 751–756 (1972).
14. T. Kita and T. Harada, "Ruling engine using a piezoelectric device for large and high-groove density gratings," Appl. Opt. **31**, 1399–1406 (1992).
15. C. Yang, H. Yu, S. Jiang, X. Li, X. Qi, Bayanheshig, and Y. Tang, "Influence of running accuracy of ruling carriage system on grating spectrum performance," Opt. Precis. Eng. **22**, 2674–2682 (2014).